J Oral Pathol Med (2004) 33: 185–90
© Blackwell Munksgaard 2004 · All rights reserved
www.blackwellmunksgaard.com/jopm

Expression of Sonic hedgehog (SHH) signaling molecules in ameloblastomas

Hiroyuki Kumamoto, Kousuke Ohki, Kiyoshi Ooya

Division of Oral Pathology, Department of Oral Medicine and Surgery, Tohoku University Graduate School of Dentistry, Sendai, Japan

BACKGROUND: To clarify the roles of Sonic hedgehog (SHH) signal transduction in oncogenesis and cytodifferentiation of odontogenic tumors, expression of SHH, Patched (PTC), Smoothened (SMO), and GLI1 was analyzed in ameloblastomas as well as in tooth germs.
METHODS: Tissue specimens of 9 tooth germs, 36 benign ameloblastomas, and 1 malignant ameloblastoma were examined by reverse transcriptase-polymerase chain reaction (RT-PCR) and immunohistochemistry for the expression of SHH, PTC, SMO, and GLI1.
RESULTS: Expression of SHH, PTC, SMO, and GLI1 mRNA was detected in all tooth germ and ameloblastoma samples. Immunohistochemical reactivity for SHH, PTC, SMO, and GLI1 was detected in both normal and neoplastic odontogenic tissues. Expression of SHH, PTC, and GLI1 was more evident in epithelial cells than in mesenchymal cells, whereas SMO reactivity was marked in both epithelial and mesenchymal components in tooth germs and ameloblastomas. In ameloblastomas, these SHH signaling molecules were expressed more intensely in peripheral columnar or cuboidal cells than in central polyhedral cells; keratinizing cells and granular cells showed no or little reactivity.
CONCLUSION: Expression of SHH, PTC, SMO, and GLI1 in tooth germs and ameloblastomas suggests that these SHH signaling molecules might play a role in epithelial–mesenchymal interactions and cell proliferation in tooth development as well as in growth of these epithelial odontogenic tumors.
J Oral Pathol Med (2004) **33**: 185–90

Keywords: ameloblastoma; GLI1; Patched (PTC); Smoothened (SMO); Sonic hedgehog (SHH)

Correspondence: Hiroyuki Kumamoto, Division of Oral Pathology, Department of Oral Medicine and Surgery, Tohoku University Graduate School of Dentistry, 4-1 Seiryo-machi, Aoba-ku, Sendai 980-8575, Japan. Tel.: +81 22 717 8303. Fax: +81 22 717 8304. E-mail: kumamoto@mail.tains.tohoku.ac.jp
Accepted for publication September 10, 2003

Introduction

Tumors arising from epithelium of the odontogenic apparatus or from its derivatives or remnants exhibit considerable histologic variation and are classified into several benign and malignant entities (1–4). Ameloblastoma is the most frequently encountered tumor arising from odontogenic epithelium and is characterized by a benign but locally invasive behavior with a high risk of recurrence (1, 2, 4). Histologically, ameloblastoma shows considerable variation, including follicular, plexiform, acanthomatous, granular cell, basal cell, and desmoplastic types (1). Malignant ameloblastoma is defined as a neoplasm in which the pattern of an ameloblastoma and cytologic features of malignancy are shown by the primary growth in the jaws and/or by any metastatic growth (1). Recently, malignant ameloblastoma has been subclassified into metastasizing ameloblastoma and ameloblastic carcinoma on the basis of metastatic spread and cytologic malignant features (3). Several recent studies have detected genetic and cytogenetic alterations in these epithelial odontogenic tumors (5–8); however, the detailed mechanisms of oncogenesis, cytodifferentiation, and tumor progression remain unknown.

Sonic hedgehog (*SHH*) is a mammalian homolog of *Drosophila* segment polarity gene, *hedgehog* (*Hh*), and encodes a secreted protein that activates a membrane-receptor complex formed by Patched (PTC) and Smoothened (SMO) (9, 10). PTC is a membrane-bound protein with 12 transmembrane domains (11), and SMO is another membrane-bound protein with seven transmembrane domains and characteristics of G protein-coupled receptors (12). PTC inhibits SMO in the absence of SHH, whereas binding of SHH to PTC suspends this inhibition, thereby activating a transcriptional factor, GLI1 (10). A zinc finger DNA-binding protein, GLI1, mediates SHH signals from cytoplasm to nucleus (10, 13). SHH signal transduction plays a central role in the patterning of the limb, axial skeleton, central nervous system, lungs, digestive tract, dermal appendages, and teeth (14–17). Inherited or sporadic alterations in SHH-signaling pathway genes have been implicated in a number of developmental defects, and aberrant activation of SHH-signaling pathway during adult life has resulted in tumor formation (18–25).

Our previous studies confirmed cellular kinetics, including proliferation and cell death modulators, in tooth germs

Table 1 Primers and antibodies

	Primer			*Antibody*		
	Sequence (5′–3′)	*Anneal (°C)*	*Product (bp)*	*Clonality*	*Source*	*Dilution*
SHH	Forward: GAAGATCTCCAGAAACTCC Reverse: TCGTAGTGCAGAGACTCC	57	233	Polyclonal (Goat IgG)	Santa Cruz Biotechnology Santa Cruz, CA, USA	1 : 100
PTC	Forward: TCCCAAGCAAATGTACGAGCA Reverse: TGAGTGGAGTTCTGTGCGACAC	55	144	Polyclonal (Goat IgG)	Santa Cruz Biotechnology	1 : 100
SMO	Forward: CTGGTACGAGGACGTGGAGG Reverse: AGGGTGAAGAGCGTGCAGAG	55	140	Polyclonal (Goat IgG)	Santa Cruz Biotechnology	1 : 80
GLI1	Forward: CAGAGAATGGAGCATCCTCC Reverse: TTCTGGCTCTTCCTGTAGCC	55	412	Polyclonal (Goat IgG)	Santa Cruz Biotechnology	1 : 100
GAPDH	Forward: GGAGTCAACGGATTTGGT Reverse: GTGATGGGATTTCCATTGAT	55	206			

and ameloblastomas, suggesting that these factors are associated with oncogenesis or cytodifferentiation of odontogenic epithelium (26–31). Alterations of *PTC* have been studied in odontogenic keratocysts (32, 33); however, investigations of SHH signaling molecules in odontogenic tumors are scant (5, 34). In the present study, expression of SHH, PTC, SMO, and GLI1 was examined in ameloblastomas as well as in tooth germs using reverse transcriptase-polymerase chain reaction (RT-PCR) and immunohistochemistry to clarify the possible role of SHH signal transduction in epithelial odontogenic tumors.

Materials and methods

The study protocol was reviewed and approved by the Research Ethics Committee of Tohoku University Graduate School of Dentistry.

Tissue preparation

Specimens were surgically removed from 37 patients with ameloblastoma at the Department of Oral and Maxillofacial Surgery, Tohoku University Dental Hospital. The tumors were divided into several parts. The first part was fixed in 4% paraformaldehyde phosphate buffer for one to several days and was embedded in paraffin. The tissue blocks were sliced and stained with hematoxylin and eosin for histologic diagnosis according to the WHO histologic typing of odontogenic tumors (4). The tumors comprised 36 ameloblastomas and 1 malignant ameloblastoma. The ameloblastomas were divided into 24 follicular and 12 plexiform types, including 12 acanthomatous and 2 granular cell subtypes. The malignant ameloblastoma was compatible with a metastasizing ameloblastoma according to the criteria provided by Eversole (3). The second part of each tumor was immediately frozen on dry ice and stored at −80°C until RT-PCR analysis. The third part of each tumor was embedded in Tissue-Tek OCT Compound (Sakura Finetechnical, Tokyo, Japan), quick-frozen in a mixture of acetone and dry ice, and stored at −80°C until immunohistochemical examination. Tooth germs of the mandibular third molars, enucleated from nine patients for orthodontic reasons at the stage of crown mineralization, were similarly prepared and compared with the ameloblastomas.

RT-PCR

Total RNA was extracted from each frozen tissue using an RNeasy Mini Kit (Qiagen, Hilden, Germany) according to the manufacturer's protocol. First-stranded complementary DNA (cDNA) was synthesized from 1 μg of RNA using an Omniscript RT Kit (Qiagen) with oligo-$(dT)_{15}$ primer (Roche Diagnostics, Mannheim, Germany) as outlined by the manufacturer. The cDNA samples were amplified using a HotstarTaq Master Mix Kit (Qiagen) with specific primers in a DNA thermal cycler (Eppendorf, Hamburg, Germany). Primers used for detection of SHH, PTC, SMO, and GLI1 are listed in Table 1. A housekeeping gene, glyceraldehyde-3-phosphate dehydrogenase (GAPDH), was used as an internal control for the examination of human gene expression. PCR was performed in a total volume of 50 μl, containing 0.5 μg of template cDNA and 0.5 μM of each specific primer set. The procedure for amplification included 35 cycles of denaturation at 94°C for 45 s, annealing at 57°C (for SHH) or 55°C (for PTC, SMO, GLI1, and GAPDH) for 45 s and elongation at 72°C for 60 s with heat starting at

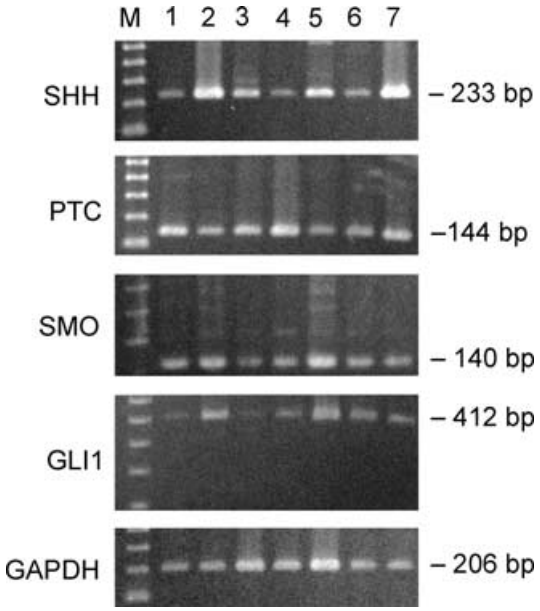

Figure 1 RT-PCR analysis of SHH, PTC, SMO, and GLI1 mRNA expression in tooth germs and ameloblastomas (M: molecular-weight standard; 1, 2: tooth germs; 3–6: ameloblastomas; and 7: malignant ameloblastoma). SHH, PTC, SMO, and GLI1 mRNA expression was seen in all samples. GAPDH was run as a control to ascertain the integrity of mRNA/cDNA. The sizes of SHH, PTC, SMO, GLI1, and GAPDH PCR products were 233, 144, 140, 412, and 206 bp, respectively.

95°C for 15 min and final elongation at 72°C for 10 min. The PCR products were electrophoresed on 2% agarose gel at 100 V for 40 min and visualized with ethidium bromide.

Immunohistochemistry

Serial cryostat sections each of 5 μm thick were obtained from each frozen block. The sections were fixed in cold acetone for 10 min and washed in cold phosphate-buffered saline (PBS). After treatment with normal rabbit serum for 30 min, the sections were incubated with primary monoclonal antibodies at 4°C overnight. The applied antibodies are listed in Table 1. The standard streptavidin–biotin–peroxidase complex method was performed to bind the primary antibodies with the use of a Histofine SAB-PO Kit (Nichirei, Tokyo, Japan). Reaction products were visualized by immersing the sections for 1–3 min in 0.03% diaminobenzidine solution containing 2 mM hydrogen peroxide. Nuclei were lightly counterstained with methylgreen. For control studies of the antibodies, the serial sections were treated with PBS and normal goat IgG instead of the primary antibodies and were confirmed to be unstained.

Evaluation of immunostaining and statistical analysis

Immunohistochemical reactivity for SHH, PTC, SMO, and GLI1 was evaluated and classified into three groups: (−) negative, (+) positive, and (++) strongly positive. The statistical significance of differences in the percentages of cases with different reactivity levels was analyzed by the Mann–Whitney *U*-test for differences between two groups or the Kruskal–Wallis test for differences among three groups. *P*-values of less than 0.05 were considered to indicate statistical significance.

Results

SHH, PTC, SMO, and GLI1 mRNA expression

RT-PCR analysis identified expression of mRNA transcripts for SHH, PTC, SMO, and GLI1 in all 36 ameloblastomas and 1 malignant ameloblastoma as well as in the nine tooth germ tissues (Fig. 1). The PCR products of SHH, PTC, SMO, and GLI1 were 233, 144, 140, and 412 bp, respectively. There was no distinct difference in SHH, PTC, SMO, and GLI1 mRNA expression among the different types of ameloblastomas or between the malignant and benign ameloblastomas.

Immunohistochemical reactivity for SHH, PTC, SMO, and GLI1

Immunohistochemical reactivity for SHH, PTC, SMO, and GLI1 was detected in the cytoplasm of cellular components

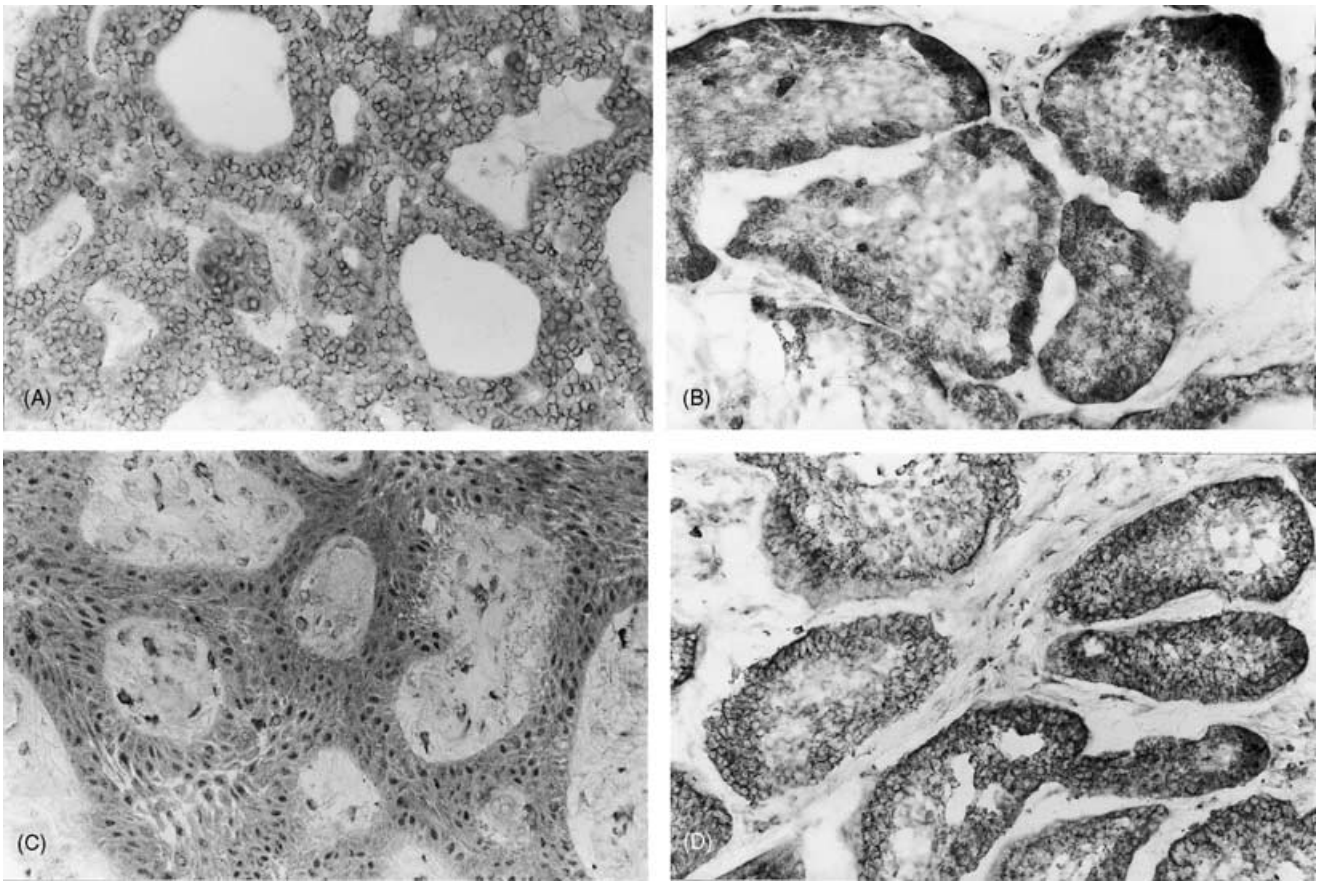

Figure 2 Immunohistochemical reactivity for SHH, PTC, SMO, and GLI1 in ameloblastomas. (A) Plexiform ameloblastoma showing stronger SHH reactivity in peripheral cuboidal cells than in central polyhedral cells. Stromal cells are not reactive (×190). (B) Follicular ameloblastoma showing stronger PTC reactivity in peripheral columnar cells than in central polyhedral cells. Stromal cells are weakly reactive (×185). (C) Plexiform ameloblastoma showing SMO reactivity in tumor cells and stromal fibroblasts (×155). (D) Follicular ameloblastoma showing stronger GLI1 reactivity in peripheral columnar cells than in central polyhedral cells. Stromal cells are weakly reactive (×185).

Table 2 Immunoreactivity for SHH, PTC, SMO, and GLI1 in tooth germs and ameloblastomas

	SHH			*PTC*			*SMO*			*GLI1*		
	(−)	*(+)*	*(++)*	*(−)*	*(+)*	*(++)*	*(−)*	*(+)*	*(++)*	*(−)*	*(+)*	*(++)*
Tooth germ ($n=9$)												
Dental lamina	0 (0)	2 (40)	3 (60)	0 (0)	0 (0)	5 (100)	0 (0)	1 (20)	4 (80)	0 (0)	1 (20)	4 (80)
Dental follicle/papilla	0 (0)	9 (100)	0 (0)	9 (100)	0 (0)	0 (0)	0 (0)	2 (22)	7 (78)	0 (0)	9 (100)	0 (0)
Ameloblastoma ($n=36$)												
Tumor cells	0 (0)	11 (31)	25 (69)	0 (0)	9 (25)	27 (75)	0 (0)	21 (58)	15 (42)	0 (0)	9 (25)	27 (75)
Stromal cells	8 (22)	28 (78)	0 (0)	0 (0)	30 (83)	6 (17)	0 (0)	10 (28)	26 (72)	0 (0)	27 (75)	9 (25)
Follicular type ($n=24$)												
Tumor cells	0 (0)	6 (25)	18 (75)	0 (0)	7 (29)	17 (71)	0 (0)	13 (54)	11 (46)	0 (0)	6 (25)	18 (75)
Stromal cells	4 (17)	20 (83)	0 (0)	0 (0)	20 (83)	4 (17)	0 (0)	8 (33)	16 (67)	0 (0)	17 (71)	7 (29)
Plexiform ($n=12$)												
Tumor cells	0 (0)	5 (42)	7 (58)	0 (0)	2 (17)	10 (83)	0 (0)	8 (67)	4 (33)	0 (0)	3 (25)	9 (75)
Stromal cells	4 (33)	8 (67)	0 (0)	0 (0)	10 (83)	2 (17)	0 (0)	2 (17)	10 (83)	0 (0)	10 (83)	2 (17)
Acanthomatous subtype ($n=12$)												
Tumor cells	0 (0)	2 (17)	10 (83)	0 (0)	2 (17)	10 (83)	0 (0)	7 (58)	5 (42)	0 (0)	2 (17)	10 (83)
Stromal cells	3 (25)	9 (75)	0 (0)	0 (0)	10 (83)	2 (17)	0 (0)	6 (50)	6 (50)	0 (0)	11 (92)	1 (8)
Granular subtype ($n=2$)												
Tumor cells	0 (0)	0 (0)	2 (100)	0 (0)	0 (0)	2 (100)	0 (0)	1 (50)	1 (50)	0 (0)	0 (0)	2 (100)
Stromal cells	0 (0)	2 (100)	0 (0)	0 (0)	1 (50)	1 (50)	0 (0)	0 (0)	2 (100)	0 (0)	1 (50)	1 (50)
Malignant ameloblastoma ($n=1$)												
Tumor cells	0 (0)	0 (0)	1 (100)	0 (0)	0 (0)	1 (100)	0 (0)	1 (100)	0 (0)	0 (0)	0 (0)	1 (100)
Stromal cells	0 (0)	1 (100)	0 (0)	0 (0)	1 (100)	0 (0)	0 (0)	0 (0)	1 (100)	0 (0)	1 (100)	0 (0)

Immunohistochemical reactivity: (−), negative; (+), positive; and (++), strongly positive.
Values in parentheses denote percentage values.

in both normal and neoplastic odontogenic tissues (Fig. 2; Table 2). In tooth germs, expression of SHH, PTC, and GLI1 was more evident in epithelial cells of the dental laminae than in mesenchymal cells of the dental follicles and dental papillae, and SMO reactivity was marked in both epithelial and mesenchymal cells. Ameloblastomas showed stronger expression of SHH, PTC, SMO, and GLI1 in peripheral columnar or cuboidal cells than in central polyhedral cells (Fig. 2). In acanthomatous and granular cell ameloblastomas, keratinizing cells and granular cells showed no or little reactivity for these molecules. SMO expression was markedly found in stromal fibroblasts as well as neoplastic cells. Immunoreactivity for SHH, PTC, and GLI1 was weak in stromal cells, and SHH reactivity in stromal cells was not recognized in 8 of 28 ameloblastomas. The malignant (metastasizing) ameloblastoma showed SHH, PTC, SMO, and GLI1 expression patterns similar to those of the benign ameloblastomas. Differences in the immunohistochemical detection of SHH, PTC, SMO, and GLI1 did not reach statistical significance.

Discussion

Sonic hedgehog signals control cell–cell interactions and cell proliferation in tissue patterning during development, and SHH signal transduction is pivotal to embryonic development (14, 15). Targeted gene disruption of *Shh* in mice results in abnormal development of the brain, spinal cord, axial skeleton, and limbs (35). In humans, holoprosencephaly with cyclopia has been attributed to germline mutations with *SHH* (23). Expression of SHH and its signaling molecules have been detected temporally and spatially during tooth development, indicating a role in early tooth germ initiation and subsequent epithelial–mesenchymal interactions (15–17). In the present study, SHH, PTC, SMO, and GLI1 expression was detected in epithelial and mesenchymal components of human tooth germ tissues in various degrees, suggesting that these molecules are associated with epithelial–mesenchymal interactions during tooth development. Transgenic mice overexpressing *Shh* develop many kinds of tumors, such as basal cell carcinoma, medulloblastoma, and breast carcinoma, suggesting a role of *Shh* in oncogenesis (36). Some human basal cell carcinoma and lung squamous cell carcinoma tissues have shown SHH overexpression (24, 37, 38). In the present study, expression of SHH was detected predominantly in neoplastic cells in benign and metastasizing ameloblastomas. Recently, Heikinheimo et al. (5) have demonstrated by means of a cDNA microarray that the gene transcript for SHH is underexpressed in ameloblastomas. Our results showed that SHH expression in stromal cells of ameloblastomas tended to be low as compared with that in mesenchymal cells of tooth germs.

Germline mutations of *PTC* have been identified to be responsible for basal cell nevus syndrome (BCNS), an autosomal dominant hereditary disease characterized by a variety of clinical problems, including basal cell carcinomas, odontogenic keratocysts, palmar, or plantar pits, ectopic calcification, a spectrum of congenital skeletal anomalies, and various low-frequency neoplasms, such as medulloblastoma and meningioma (21, 22). Homozygous *Ptc* knockout mice die *in utero* during early organogenesis, while heterozygous *Ptc* knockout mice show a number of developmental abnormalities and a high incidence of tumors, similar to human BCNS (39–41). Recent studies have demonstrated somatic

mutations of *PTC* and/or deletions of chromosome 9q22.3, *PTC* locus, in some sporadic tumors, such as basal cell carcinoma, trichoepithelioma, medulloblastoma, meningioma, breast carcinoma, and esophageal carcinoma as well as in patients with BCNS (20, 42–44). *PTC* mutations and deletions of *PTC* locus have been identified in both BCNS-associated and sporadic odontogenic keratocysts (32, 33). Barreto et al. (34) have detected immunoreactivity for PTC protein in ameloblastomas, suggesting that the SHH-signaling pathway might be activated in these odontogenic tumors. In the present study, benign and metastasizing ameloblastomas showed stronger PTC expression in neoplastic cells than in stromal cells, and epithelial PTC expression in ameloblastomas tended to be low as compared with that in tooth germs.

SMO and *GLI1* have been shown to have oncogenic potential (18, 19). Missense mutations of *SMO* have been recognized in sporadic basal cell carcinoma and medulloblastoma, and basal cell carcinoma has shown expression of SMO transcript and protein (25, 38). Transgenic mice overexpressing mutant *Smo* have induced basal cell carcinoma (45). Overexpression of GLI1 has been demonstrated in human basal cell carcinoma, medulloblastoma, glioma, and prostate carcinoma (19, 24), and mice overexpressing *Gli1* have developed basal cell carcinoma as well as other hair follicle-derived tumors, such as trichoepithelioma, cylindroma, and trichoblastoma (46). In the present study, benign and metastasizing ameloblastomas showed SMO and GLI1 expression in neoplastic and stromal cells, and reactivity for GLI1 was more evident in neoplastic cells than in stromal cells. Epithelial SMO expression in these epithelial odontogenic tumors tended to be low as compared with that in dental laminae, and stromal GLI1 reactivity in ameloblastomas was slightly higher than mesenchymal GLI1 reactivity in tooth germs. Our examinations detected expression of SHH, PTC, SMO, and GLI1 in benign and metastasizing ameloblastomas at mRNA and protein levels, suggesting that these SHH signaling molecules may play a role in epithelial–mesenchymal interactions and cell proliferation during growth of these epithelial odontogenic tumors. Our results showed no statistically significant difference between normal or neoplastic odontogenic tissues or among the different types of ameloblastomas, and did not clearly indicate that SHH signal transduction had a specific role in oncogenesis of odontogenic epithelium. Further genetic studies of these SHH signaling molecules in odontogenic tumors are needed to establish potential associations between SHH signaling and oncogenesis of odontogenic epithelium.

References

1. Kramer IRH, Pindborg JJ, Shear M. *WHO Histological Typing of Odontogenic Tumours*. Berlin: Springer-Verlag, 1992; 11–27.
2. Melrose RJ. Benign epithelial odontogenic tumors. *Semin Diagn Pathol* 1999; **16**: 271–87.
3. Eversole LR. Malignant epithelial odontogenic tumors. *Semin Diagn Pathol* 1999; **16**: 317–24.
4. Sciubba JJ, Fantasia JE, Kahn LB. *Tumors and Cysts of the Jaw*. Washington, DC: Armed Forces Institute of Pathology, 2001; 71–99.
5. Heikinheimo K, Jee KJ, Niini T, et al. Gene expression profiling of ameloblastoma and human tooth germ by means of a cDNA microarray. *J Dent Res* 2002; **81**: 525–30.
6. Jääkeläinen K, Jee KJ, Leivo I, Saloniemi I, Knuutila S, Heikinheimo K. Cell proliferation and chromosomal changes in human ameloblastoma. *Cancer Genet Cytogenet* 2002; **136**: 31–7.
7. Sandra F, Nakamura N, Kanematsu T, Harata M, Ohishi M. The role of MDM2 in the proliferative activity of ameloblastoma. *Oral Oncol* 2002; **38**: 163–7.
8. Shibata T, Nakata D, Chiba I, et al. Detection of TP53 mutation in ameloblastoma by the use of a yeast functional assay. *J Oral Pathol Med* 2002; **31**: 534–8.
9. Nüsslein-Vohhard C, Wieschaus E. Mutations affecting segment number and polarity in *Drosophila*. *Nature* 1980; **287**: 795–801.
10. Ingham PW, McMahon AP. Hedgehog signaling in animal development: paradigms and principles. *Genes Dev* 2001; **15**: 3059–87.
11. Stone DM, Hynes M, Armanini M, et al. The tumour-suppressor gene *patched* encodes a candidate receptor for Sonic hedgehog. *Nature* 1996; **384**: 129–34.
12. Alcedo J, Ayzenzon M, Von Ohlen T, Noll M, Hooper JE. The *Drosophila smoothened* gene encodes a seven-pass membrane protein, a putative receptor for the Hedgehog signal. *Cell* 1996; **86**: 221–32.
13. Alexandre C, Jacinto A, Ingham PW. Transcriptional activation of *hedgehog* target genes in *Drosophila* is mediated directly by the Cubitus interruptus protein, a member of the GLI family of zinc finger DNA-binding proteins. *Genes Dev* 1996; **10**: 2003–13.
14. Echelard Y, Epstein DJ, St-Jacques B, et al. Sonic hedgehog, a member of a family of putative signaling molecules, is implicated in the regulation of CNS polarity. *Cell* 1993; **75**: 1417–30.
15. Bitgood MJ, McMahon AP. *Hedgehog* and *Bmp* genes are coexpressed at many diverse sites of cell–cell interaction in the mouse embryo. *Dev Biol* 1995; **172**: 126–38.
16. Dassule HR, McMahon AP. Analysis of epithelial–mesenchymal interactions in the initial morphogenesis of the mammalian tooth. *Dev Biol* 1998; **202**: 215–27.
17. Hardcastle Z, Mo R, Hui C, Sharpe PT. The Shh signaling pathway in tooth development. defects in *Gli2* and *Gli3* mutants. *Development* 1998; **125**: 2803–11.
18. Hahn H, Wojnowski L, Miller G., Zimmer A. The patched signaling pathway in tumorigenesis and development: lessons from animal models. *J Mol Med* 1999; **77**: 459–68.
19. Altaba AR, Sánchez P, Dahmane N. Gli and Hedgehog in cancer: tumours, embryos and stem cells. *Nat Rev Cancer* 2002; **2**: 361–72.
20. Gailani MR, Ståhle-Bäckdahl M, Leffell DJ, et al. The role of the human homologue of *Drosophila patched* in sporadic basal cell carcinomas. *Nat Genet* 1996; **14**: 78–81.
21. Hahn H, Wicking C, Zaphiropoulos PG, et al. Mutations of the human homolog of *Drosophila patched* in the nevoid basal cell carcinoma syndrome. *Cell* 1996; **85**: 841–51.
22. Johnson RL, Rothman AL, Xie J, et al. Human homolog of *patched*, a candidate gene for the basal cell nevus syndrome. *Science* 1996; **272**: 1668–71.
23. Roessler E, Belloni E, Gaudenz K, et al. Mutations human *Sonic hedgehog* gene cause holoprosencephaly. *Nat Genet* 1996; **14**: 357–60.
24. Dahmane N, Lee J, Robins P, Heller P, Altaba AR. Activation of the transcription factor Gli1 and the Sonic hedgehog signaling pathway in skin tumours. *Nature* 1997; **389**: 876–81.

25. Reifenberger J, Wolter M, Weber RG, et al. Missense mutations in *SMOH* in sporadic basal cell carcinomas of the skin and primitive neuroectodermal tumors of the central nervous system. *Cancer Res* 1998; **58**: 1798–803.
26. Kumamoto H. Detection of apoptosis-related factors and apoptotic cells in ameloblastomas. analysis by immunohistochemistry and an *in situ* DNA nick end-labelling method. *J Oral Pathol Med* 1997; **26**: 419–25.
27. Kumamoto H, Ooya K. Immunohistochemical analysis of bcl-2 family proteins in benign and malignant ameloblastomas. *J Oral Pathol Med* 1999; **28**: 343–9.
28. Kumamoto H, Kimi K, Ooya K. Detection of cell cycle-related factors in ameloblastomas. *J Oral Pathol Med* 2001; **30**: 309–15.
29. Kumamoto H, Kimi K, Ooya K. Immunohistochemical analysis of apoptosis-related factors (Fas, Fas ligand, caspase-3 and single-stranded DNA) in ameloblastomas. *J Oral Pathol Med* 2001; **30**: 596–602.
30. Kumamoto H, Kinouchi Y, Ooya K. Telomerase activity and telomerase reverse transcriptase (TERT) expression in ameloblastomas. *J Oral Pathol Med* 2001; **30**: 231–6.
31. Kumamoto H, Yoshida M, Ooya K. Immunohistochemical detection of hepatocyte growth factor, transforming growth factor-β and their receptors in epithelial odontogenic tumors. *J Oral Pathol Med* 2002; **31**: 539–48.
32. Lench NJ, High AS, Mark ham AF, Hume WC, Robinson PA. Investigation of chromosome 9q22.3-q31 DNA marker loss in odontogenic keratocysts. *Oral Oncol Eur J Cancer* 1996; **32B**: 202–6.
33. Levanat S, Gorlin RJE, Fallen S, Johnson DR, Fantasia JED, Bale AE. A two-hit model for developmental defects in Gorlin syndrome. *Nat Genet* 1996; **12**: 85–7.
34. Barreto DC, Bale AE, De Marco L, Gomen RS. Immunolocalization of PATCH protein in odontogenic cysts and tumors. *J Dent Res* 2002; **81**: 757–60.
35. Chiang C, Litingtung Y, Lee E, et al. Cyclopia and defective axial patterning in mice lacking *Sonic hedgehog* gene function. *Nature* 1996; **383**: 407–13.
36. Oro AE, Higgins KM, Hu Z, Bonifas JM, Epstein EH, Jr, Scott MP. Basal cell carcinomas in mice overexpressing Sonic hedgehog. *Science* 1997; **276**: 817–21.
37. Fujita E, Khoroku Y, Urase K, et al. Involvement of *Sonic hedgehog* in the cell growth of LK-2 cells, human lung squamous carcinoma cells. *Biochem Biophys Res Commun* 1997; **238**: 658–64.
38. Kallassy M, Toftgård R, Ueda M, et al. Patched (*ptch*)-associated preferential expression of smoothened (*smoh*) in human basal cell carcinoma of the skin. *Cancer Res* 1997; **57**: 4731–5.
39. Goodrich LV, Milenkovic L, Higgins KM, Scott MP. Altered neural cell fates and medulloblastoma in mouse *patched* mutants. *Science* 1997; **277**: 1109–13.
40. Axzterbaum M, Epstein J, Oro A, et al. Ultraviolet and ionizing radiation enhance the growth of BCCs and trichoblastomas in patched heterozygous knockout mice. *Nat Med* 1999; **5**: 1285–91.
41. Kimi K, Ohki K, Kumamoto H, et al. Immunohistochemical and genetic analysis of mandibular cysts in heterozygous *ptc* knockout mice. *J Oral Pathol Med* 2003; **32**: 108–13.
42. Vorechovský I, Undén AB, Sandstedt B, Toftgård R, Ståhle-Bäckdahl M. Trichoepitheliomas contain somatic mutations in the overexpressed *PTCH* gene: support for a gatekeeper mechanism in skin tumorigenesis. *Cancer Res* 1997; **57**: 4677–81.
43. Xie J, Johnson RL, Zhang X, et al. Mutations of the *PATCHED* gene in several types of sporadic extracutaneous tumors. *Cancer Res* 1997; **57**: 2369–72.
44. Maesawa C, Tamura G, Iwaya T, et al. Mutations in the human homologue of the *Drosophila patched* gene in esophageal squamous cell carcinoma. *Genes Chromosomes Cancer* 1998; **21**: 276–9.
45. Xie J, Murone M, Luoh S-M, et al. Activating *Smoothened* mutations in sporadic basal-cell carcinoma. *Nature* 1998; **391**: 90–2.
46. Nilsson M, Undén AB, Krause D, et al. Induction of basal cell carcinomas and trichoepitheliomas in mice overexpressing GLI-1. *Proc Natl Acad Sci USA* 2000; **97**: 3438–43.

This document is a scanned copy of a printed document. No warranty is given about the accuracy of the copy. Users should refer to the original published version of the material.